JACS
JOURNAL OF THE AMERICAN CHEMICAL SOCIETY
Article
pubs.acs.org/JACS

Efficient Greenish Blue Electrochemiluminescence from Fluorene and Spirobifluorene Derivatives

Federico Polo,*[,†,∥] Fabio Rizzo,*[,‡,§] Manoel Veiga-Gutierrez,[†] Luisa De Cola,[†] and Silvio Quici[‡,§]

[†]Physikalisches Institut, Westfälische Wilhelms-Universität, Heisenbergstrasse 11, D-48149 Münster, Germany
[‡]Istituto di Scienze e Tecnologie Molecolari (ISTM), CNR, Via Golgi 19, I-20133 Milano, Italy
[§]Polo Scientifico Tecnologico (PST), CNR, Via Fantoli 16/15, I-20138 Milano, Italy

Supporting Information

ABSTRACT: The spectroscopic and electrochemical behavior as well as electrogenerated chemiluminescence (ECL) of a series of donor−π−donor derivatives bearing triphenylamine groups as donor connected to a fluorene, 2,7-bis-(4-(*N*,*N*-diphenylamino)phen-1-yl)-9,9′-dimethylfluorene (**1**), or spirobifluorene core, 2,7-bis-(4-(*N*,*N*-diphenylamino)phen-1-yl)-9,9′-spirobifluorene (**2**) and 2,2′,7,7′-tetrakis(4-(*N*,*N*-diphenylamino)phen-1-yl)-9,9′-spirobifluorene (**3**), were investigated. Besides a high photoluminescence (PL) quantum yield in solution (between 81 and 87%), an efficient radical ions annihilation process induces intense greenish blue ECL emission that could be seen with the naked eye. Only the tetrasubstituted spirobifluorene derivative (compound **3**) shows weak ECL obtained by a direct annihilation mechanism. Because the energy of the annihilation reaction is higher than the energy required to form the singlet excited state, the S-route could be considered the pathway followed by the ECL process in these molecules. The ECL emissions recorded by direct ion−ion annihilation show two bands compared to the single structureless PL band. The ECL spectra obtained by a coreactant approach using benzoylperoxide as a coreagent show no differences relative to that produced by annihilation, except for an increasing of ECL intensity for all compounds.

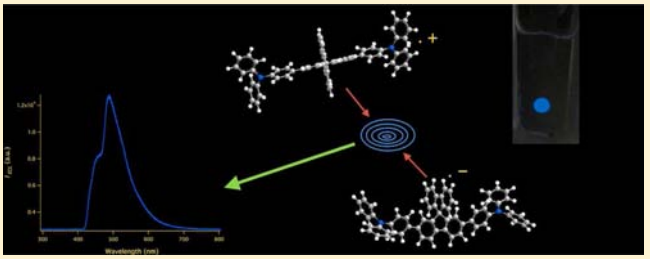

INTRODUCTION

Electrogenerated chemiluminescence (or electrochemiluminescence, ECL) is a very sensitive technique that can be used to investigate radical ion formation and the luminescence produced by annihilation reactions between radical cations and anions, generated during electrochemical oxidation and reduction processes.[1] Although this technique is similar to the photoexcitation method, it has the advantage that a light source is not employed, thus avoiding the scattering phenomenon.[2] Since the light intensity is usually proportional to the concentration of the emitting species, ECL has found a very wide application in diagnostics as a powerful analytical tool.[3] The ECL mechanism can involve excited singlet state formation by direct annihilation as follows:

$$R - e \rightarrow R^{\bullet +} \quad \text{(radical cation formation)} \tag{1}$$

$$R + e \rightarrow R^{\bullet -} \quad \text{(radical anion formation)} \tag{2}$$

$$R^{\bullet +} + R^{\bullet -} \rightarrow {}^1R^* + R \quad \text{(excited singlet state formation)} \tag{3}$$

$${}^1R^* \rightarrow R + h\nu \quad \text{(ECL emission)} \tag{4}$$

where R is the electroactive species. This pathway is defined as the "S-route" because the singlet is directly generated (eq 3) in systems with sufficient energy. Systems with insufficient energy instead follow the "T-route" in which the triplet state is first produced (eq 5), and then the subsequent triplet−triplet annihilation generates the singlet excited state $^1R^*$ (eq 6) that emits light (eq 4).[4]

$$R^{\bullet +} + R^{\bullet -} \rightarrow {}^3R^* + R \quad \text{(excited triplet state formation)} \tag{5}$$

$${}^3R^* + {}^3R^* \rightarrow {}^1R^* + R \quad \text{(triplet−triplet annihilation)} \tag{6}$$

Alternatively to S- and T-routes, ion annihilation reactions can lead to direct formation of excimers or exciplexes:

$$R^{\bullet +} + R^{\bullet -} \rightarrow R^*_2 \quad \text{(excimer formation)} \tag{7}$$

$$R^{\bullet +} + R'^{\bullet -} \rightarrow (RR')^* \quad \text{(exciplex formation)} \tag{8}$$

Another ECL pathway involves adding a reagent (or coreactant) that can produce a strong reducing or strong oxidizing agent, depending on its nature. For example, benzoyl peroxide (BPO) is a commonly used coreactant. Upon reduction, BPO decomposes to form a strong oxidizing agent (E^{ox} = +1.5 V vs saturated calomel electrode (SCE)),[4,5] which can react with the radical anion to produce the excited state:

Received: June 4, 2012
Published: August 9, 2012

   dx.doi.org/10.1021/ja3054018 | J. Am. Chem. Soc. 2012, 134, 15402−15409

Scheme 1. Synthetic Routes To Obtain 1−3

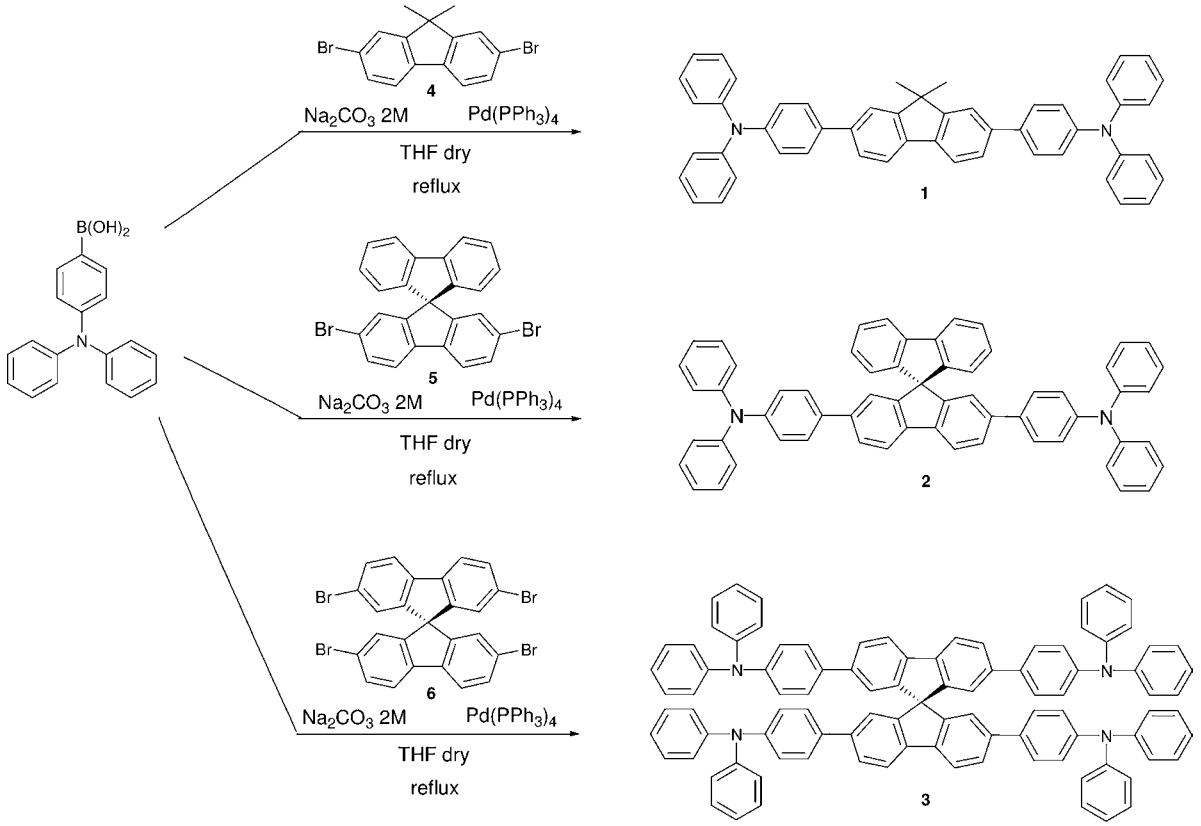

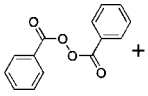

$$+ e \longrightarrow [BPO]^{\bullet -} \longrightarrow C_6H_5CO_2^{\bullet} + C_6H_5CO_2^{-} \quad (9)$$

$$C_6H_5CO_2^{\bullet} + R^{\bullet -} \rightarrow R^{*} + C_6H_5CO_2^{-} \quad (10)$$

$$R^{*} \rightarrow R + h\nu \quad (11)$$

The ECL quantum efficiency (ϕ_{ECL}) of many polyaromatic hydrocarbons (PAHs) and organometallic compounds has been determined by relative methods using 9,10-diphenylanthracene (DPA) or tris(2,2′-bipyridine)ruthenium(II) ($Ru(bpy)_3^{2+}$) as the standards.[6] ECL has been widely investigated in the past 40 years,[1−7] but to the best of our knowledge, only a few examples of quantum efficiency higher than that of DPA have been published.[8,9]

Among PAHs, fluorene- and spirobifluorene-based molecules have been recently studied as suitable candidates for ECL.[10] Spirobifluorene is characterized by two fluorene units connected through the spiro-carbon atom. This spatial configuration induces strong rigidity and increases the stability of the system, hampering the oxidation process occurring at position 9 of the fluorene ring. Moreover, spirobifluorene can be chemically modified, like fluorene, with donor and/or acceptor groups in order to tune the emission of the system. The high versatility of this synthetic approach was recently exploited, for example, to synthesize molecules bearing a fluorene and spirobifluorene core that show nonlinear optical[11] or high emissive properties.[12] Because of their attractive properties, spirobifluorenes have been proposed as suitable compounds in the field of optoelectronic devices, including solar cells[13] and organic light-emitting diodes.[14] The reported spirobifluorene derivatives showing ECL emission in the blue region have a low efficiency compared to DPA.[15]

Herein we report the synthesis, photophysical properties, electrochemical behavior, and greenish blue ECL of three organic compounds based on fluorene and spirobifluorene units, as shown in Scheme 1. In particular, the efficient ECL pursued by both ion annihilation and coreactant methodologies is described.

EXPERIMENTAL SECTION

Electrochemistry. Cyclic voltammetry (CV) for the spirobifluorene derivatives reported herein was performed in *N*,*N*-dimethylformamide (DMF)/0.1 M tetrabutylammonium hexafluorophosphate (TBAH). The concentration of the samples was 1.5 mM. Glassy carbon was employed as the working electrode, platinum wire as the counter electrode, and silver wire as the quasi-reference electrode (QRE). DMF (Acros, extra dry, 99.8%) was used as received without any further purification. TBAH (electrochemical grade, ≥99%, Fluka) was used as the supporting electrolyte, which was recrystallized from a 1:1 ethanol−water solution and dried at 60 °C under vacuum.

For the electrochemical experiments, a CHI750C electrochemical workstation (CH Instruments, Inc., Austin, TX) was used. The electrochemical experiments were performed in a glass cell under an Ar atmosphere. To minimize the ohmic drop between the working and the reference electrodes, feedback correction was employed. The electrochemical experiments were performed by using a homemade glassy carbon (Tokai Inc.) disk electrode (3 mm diameter). The working electrode was stored in ethanol and, before experiments, was polished with a 0.05 μm diamond suspension (Metadi Supreme diamond suspension, Buehler) and ultrasonically rinsed with ethanol for 5 min. The electrode was electrochemically activated in the background solution by means of several voltammetric cycles at 0.5 V/s between the anodic and the cathodic solvent/electrolyte discharges, until the same quality features were obtained. The reference electrode

dx.doi.org/10.1021/ja3054018 | J. Am. Chem. Soc. 2012, 134, 15402−15409

was a silver QRE, which was separated from the catholyte by a glass frit (Vycor). The reference electrode was calibrated at the end of each experiment against the ferrocene/ferricenium couple, whose formal potential is 0.464 V against the KCl SCE; in the following, all potential values will be reported against the SCE. A platinum wire served as the counter electrode.

ECL. The ECL transients were recorded using an Autolab PGSTAT101 electrochemical workstation (Metrohm, The Netherlands) coupled with a photosensor module with a photomultiplier tube (PMT, Hamamatsu, H10723-01, Japan). The pulsing potential was set to 50 mV past the peak potentials of the first oxidation and the first (and/or the second) reduction waves of the samples investigated. The pulse width was 0.3 s. The photocurrent produced by the PMT was directly converted to a voltage signal through the photosensor module and acquired by the external input channel of the analog-to-digital converter (ADC) of the Autolab. The transients and the faradic currents were managed by using the software NOVA provided with the Autolab. The ECL spectra were acquired using a calibrated electron-multiplying charge-coupled device (EM-CCD) camera (Andor Technology, Newton EM-CCD) coupled with a spectrograph (Andor Technology, Shamrock 163). A homemade glassy carbon (Tokai Inc.) disk electrode (3 mm diameter) was employed as the working electrode, which was close to (a few millimeters) and facing the PMT. The working electrode was mechanically and electrochemically cleaned as described above for the electrochemical measurements. The reference and counter electrodes employed were the same as reported above.

Spectroscopy Measurements. Suprasil quartz cells and spectrophotometric-grade solvents were employed. Absorption spectra were measured on a Varian Cary 5000 double-beam UV−vis−NIR spectrometer and baseline-corrected. Steady-state emission spectra were recorded on an Edinburgh FS920 spectrometer equipped with a 450-W xenon arc lamp, excitation and emission monochromators (1.8 nm/mm dispersion, 1800 grooves/mm blazed at 500 nm), and a Hamamatsu R928 PMT. Emission and excitation spectra were corrected for source intensity (lamp and grating) by standard correction curves.

The phosphorescence measurements at low temperature were performed in quartz tubes inserted in a liquid-nitrogen-filled quartz Dewar. The solvent used was methylcyclohexane, which forms a clear glass at 77 K. Phosphorescence spectra were measured using a gated camera and a pulsed laser excitation source. Briefly, a Nd:YAG (355 nm, fwhm 10 ns, 10 Hz, Spectra Physics) pumped an optical parametric oscillator (MOPO-FDO Spectra Physics) was used to tune the excitation wavelength (300 nm, 0.5 mJ/pulse). The generated emission was passed through a cutoff filter (375 nm) placed at 90° with respect to the excitation, directed through an optical fiber to a spectrograph (Acton), and detected by an intensified charge-coupled device camera (iCCD, Princeton Instruments). The delay between pump laser and high-voltage pulse amplifier (Princeton Instruments) used to gate iCCD was controlled by a programmable delay pulse generator (Berkeley Nucleonics). For all samples, accumulation of phosphorescence was performed in the time window from 1 to 51 ms.

RESULTS AND DISCUSSION

Synthesis. Details of the synthetic procedures and characterizations are given in the Experimental Section. Scheme 1 shows the synthesis of 2,7-bis(4-(*N*,*N*-diphenylamino)phen-1-yl)-9,9′-dimethylfluorene (**1**),[16] 2,7-bis(4-(*N*,*N*-diphenylamino)phen-1-yl)-9,9′-spirobifluorene (**2**),[17] and 2,2′,7,7′-tetrakis(4-(*N*,*N*-diphenylamino)phen-1-yl)-9,9′-spirobifluorene (**3**)[18] obtained by Suzuki reactions. The fluorene-based molecule was obtained by reacting 2,7-dibromo-9,9′-dimethylfluorene[19] with 4-(*N*,*N*-diphenylamino)phenylboronic acid in the presence of $Pd(PPh_3)_4$ as the catalyst and aqueous Na_2CO_3 as the base in THF, leading to **1** with a yield of 60% after purification by column chromatography. Compound **2** was prepared with a yield of 60% following the same procedure, using 2,7-dibromo-9,9′-spirobifluorene[20] as the starting material. Compound **3** was synthesized by a cross-coupling reaction with 62% yield, starting from the 2,2′,7,7′-tetrabromo-9,9′-spirobifluorene.[21] The purified product was obtained by washing the crude with pentane.

Electrochemistry. Figure 1 shows CVs of **1**−**3** in DMF containing 0.1 M TBAH as the supporting electrolyte. The

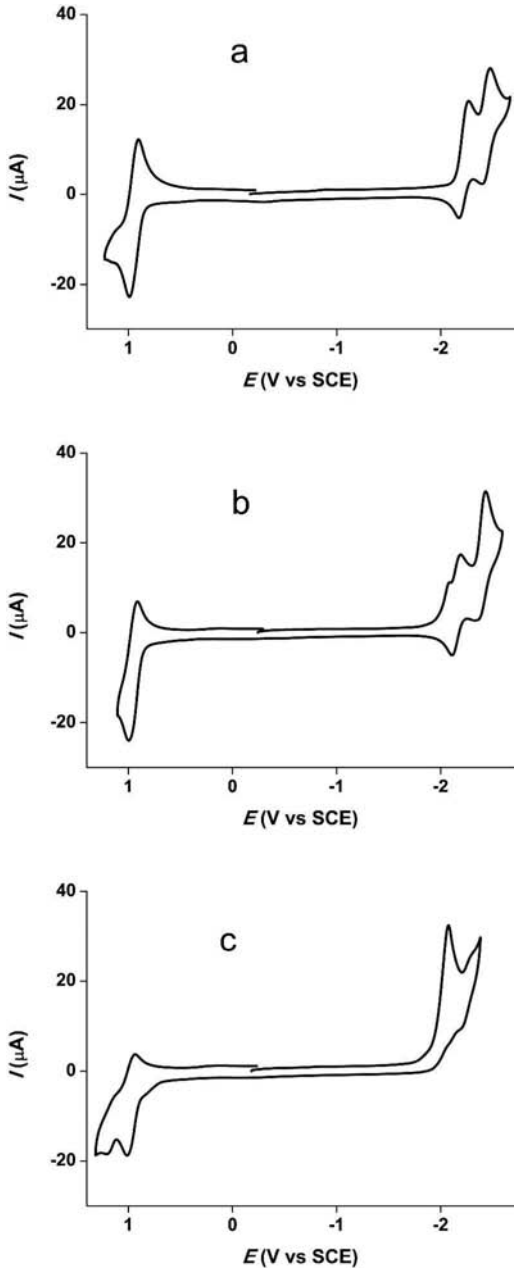

Figure 1. CVs of **1** (a), **2** (b), and **3** (c) in DMF/0.1 M TBAH. The concentration for each sample is 1.5 mM. Scan rate, 0.1 V/s; working electrode, glassy carbon; counter electrode, platinum wire; and reference electrode, silver wire.

standard potential of the redox processes was referenced against SCE and was calculated as the average value between cathodic and anodic peak potentials as the scan rate is varied in the range 0.1−5 V/s.

The CVs show only one reversible oxidation peak, attributed to the oxidation of the triphenylamines at E°_{ox} = 0.95, 0.96, and

dx.doi.org/10.1021/ja3054018 | J. Am. Chem. Soc. 2012, 134, 15402−15409

0.97 V versus SCE for **1**−**3**, respectively. The ratio between the anodic and the cathodic currents is approximately 1 down to a scan rate of 100 mV/s. By comparison with the peaks in the negative bias, integration of the peak in the positive bias reveals that the charge flowing in the oxidation process is about double the value of the reduction process. This would indicate a bielectronic process involving the simultaneous oxidation of the two amine units and can be explained by taking into account the chemical structure of the compounds. In fact, the two triphenylamine substituents are not well conjugated because of the tilted phenyl ring between the spirobifluorene (fluorene in **1**) core and the electron-donating groups. Thus, a positive charge in one triphenylamine substituent does not affect the oxidation potential of the second amine, so that they have the same value, and a single two-electron wave is observed for the oxidation.[22] On the other hand, with respect to the negative bias, by comparison of the cathodic scans for the three compounds, one can notice that **2** shows a shoulder around −2 V, followed by the formation of the radical anion as a reversible process at −2.15 V, which could be associated with the presence of the spirobifluorene core. In fact, this feature in the electrochemical pattern is missing in **1**, which is a substituted fluorene. Two reversible reduction peaks at −2.22 and −2.44 V (**1**) and at −2.15 and −2.39 V (**2**) versus SCE were observed and associated with the formation of the mono- and dianions.[23] In compound **3**, only an irreversible reduction peak was observed at −2.07 V vs SCE. The electrochemical data of all molecules are summarized in Table 1.

Table 1. Electrochemical Data in DMF/0.1 M TBAH vs SCE

compd	E_{ox} (eV)	$E_{1,red}$ (eV)	$E_{2,red}$ (eV)	ΔE (eV)
1	0.95	−2.22	−2.44	3.17
2	0.96	−2.15	−2.39	3.11
3	0.97	−2.07	–	3.04

The peak-to-peak separation was 90 mV at 0.2 V/s, which is larger than expected for an ideal Nernstian behavior (59 mV).[24] However, the behavior of the redox couple ferrocene/ferricenium ($Fc^+|Fc^0$), used as internal standard, showed the same trend. This effect can be attributed to the ohmic drop of the system, as was previously observed for aprotic media.[7a] The peak currents instead were found to be linearly dependent on the square root of the scan rate, as expected for a diffusion-controlled redox process.[24]

Spectroscopic Characterization. Absorption and emission spectra of **1**−**3** shown in Figure 2 have been recorded in the same solvent used for the electrochemical measurements for the sake of consistency, and the photophysical parameters are gathered in Table 2.

All molecules show very similar photophysical behavior. The absorption bands in the UV region can be assigned to the $\pi-\pi^*$ transitions of the entire conjugated backbone[25] with the absorption maxima occurring at 371, 374, and 375 nm for **1**−**3**, respectively. Another absorption band occurs at 300 nm for all compounds and could be attributed to the $n-\pi^*$ transition of triphenylamine groups.[26] The lack of shift in the electronic absorption profile of **2** and **3** indicates that electronic communication between the two fluorene parts is missing. Upon excitation at 350 nm, photoluminescence (PL) spectra were generated with emission maxima at 451, 456, and 462 nm for **1**−**3**, respectively. The fluorescence spectra follow the mirror-image rule with a broad, structureless band. In all three

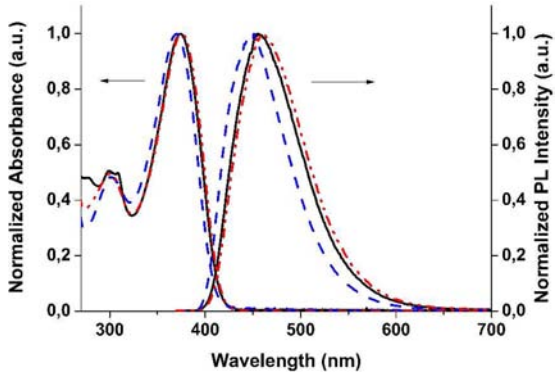

Figure 2. Absorption and emission spectra of **1** (blue dashed line), **2** (black solid line), and **3** (red dash−dot line) in DMF solutions. Excitation at 350 nm.

Table 2. Optical Data Recorded in DMF Solution

	λ_{max} (nm)					
compd	abs	PL[a]	τ_{PL} (ns)	ϕ_{PL}[b] (%)	k_r[c] (×10^8/s)	k_{nr}[c] (×10^8/s)
1	371	451	1.2	81	6.9	1.6
2	374	456	1.3	87	6.8	1.0
3	375	462	1.3	86	6.6	1.1

[a]Recorded with λ_{exc} = 350 nm. [b]Measured by integrated sphere in dichloromethane. [c]Calculated using the following equations: $k_r = \tau_{PL}/\phi_{PL}$, $k_{nr} = (1 - \phi_{PL})/\tau_{PL}$.

compounds, the nanosecond deactivation regime of the excited state is in agreement with singlet emitters, and high fluorescence quantum yields were recorded in dichloromethane by means of the integrated sphere, leading to 0.81, 0.87, and 0.86 for **1**−**3**, respectively.

ECL. Figure 3 shows the ECL spectra of **1**−**3** obtained by pulsing between the oxidation in the positive bias and the

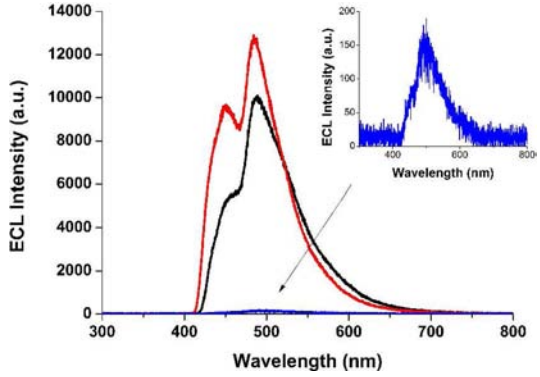

Figure 3. ECL emission spectra in DMF solution of **1** (red), **2** (black), and **3** (blue). The ECL emission scale is arbitrary, and the spectra have been offset for comparison.

second reduction peak in the negative bias (+1.2 and −2.7 V for **1**, +1.1 and −2.65 V for **2**, +1.1 and −2.5 V for **3**). Radical cations and radical anions annihilate to form an excited state whose subsequent emission signal was integrated for 5 s using a 1 nm slit width. Such a short exposition time employed to collect the ECL emission spectra suggests that the annihilation process in these molecules is highly efficient. The ECL occurring by annihilation of radical anion and cation in **1** shows two maxima, the first at 453 nm and the second at longer

dx.doi.org/10.1021/ja3054018 | J. Am. Chem. Soc. 2012, 134, 15402−15409

wavelength centered at 484 nm. In **2** the ECL emission spectrum shows a shoulder at 450 nm and an intense peak at lower energy with emission maximum at 493 nm. A similar behavior was reported by Fungo et al.[27] for a spirobifluorene bearing a single diphenylamino group as substituent. The weak ECL emission of **3** could be ascribed to the instability of the radical ions and the formation of a polymer film on the electrodic surface.

The ECL quantum yields were calculated by comparative methods as the photons emitted per redox event relative to DPA under similar conditions using DMF as solvent. For **1** and **2** we found higher quantum yields than for DPA (see Table 3).

Table 3. Photophysical and ECL Data Measured in DMF

	λ_{max} (nm)						
compd	abs	PL	ECL	E_s[b] (eV)	ΔH_{ann}[c] (eV)	ϕ_{PL}[f] (%)	ϕ_{ECL}[g]
1	371	451	453, 484	2.75	3.07,[d] 3.29[e]	81	3.0
2	374	456	450 (sh)[a], 493	2.72	3.01,[d] 3.25[e]	87	1.7
3	375	462	~490	2.68	2.94	86	–[h]

[a]sh = shoulder. [b]E_s estimated from fluorescence emission maximum. [c]$-\Delta H_{ann} = E_{ox} - E_{red} - 0.1$.[1] [d]With $E_{1,red}$. [e]With $E_{2,red}$. [f]Measured by integrated sphere in dichloromethane. [g]Relative to DPA, taking ϕ_{ECL} of DPA = 1. [h]Too weak to be measured accurately (see inset in Figure 3).

To the best of our knowledge, these are among the highest values achieved with PAHs emitting in the greenish blue region. Nevertheless, it is worth mentioning that the ECL efficiency of DPA was demonstrated to be solvent dependent.[28] However, the stability of ECL of all compounds decreased with the time, as was also observed in photocurrent decay reported in the Supporting Information (Figure S1). We hypothesized that this phenomenon is due to the formation of a thin polymer film on the electrodic surface. In fact, once the electrode was polished after this loss of ECL, the intensity of the emission was restored, corroborating the formation of a thin film over the electrode while pulsing the potential. To further investigate this phenomenon, we recorded CVs of **2** before and after pulsing the potential for several cycles between the oxidation and the second reduction potential in the positive and negative bias, respectively. The outcome, reported in Figure 4, clearly shows that the compound underwent a chemical reaction after pulsing the potential. Notably, the loss of reversibility involved both the oxidized and reduced species.

In fact, scanning the potential for several cycles around the oxidation peak (centered at $E^0 = 0.96$ V) does not produce any change. The same consideration is valid upon scanning the potential for several cycles around the first and second reduction peaks. Therefore, it can be concluded that the electropolymerization of the triphenylamine, as described in the literature,[29] does not cause the formation of secondary products. Furthermore, a similar outcome has been reported in the literature for 3,6-dispirobifluorene-*N*-phenylcarbazole.[15b] The product of the annihilation process formed an insoluble film on the electrodic surface, which altered the electrochemical behavior of the compound under investigation, thus supporting our hypothesis.

To understand which pathway is followed by ECL reaction in our systems, we calculated the energy of the excited state from the fluorescence spectrum by the equation E_s (eV) = 1239.81/λ, where λ (in nm) is the wavelength at the maximum emission peak.[8] The estimated values for the energy of the first single excited state are 2.75, 2.72, and 2.68 eV for **1**–**3**, respectively. If the annihilation energy ΔH_{ann} is higher than E_s, the system can be defined as "energy-sufficient", and the luminescence comes from a species in a singlet excited state; in this case the process is known as the singlet or S-route.[1−4] ΔH_{ann} (in eV)[1] can be calculated from the equation $-\Delta H_{ann} = E_{ox} - E_{red} - 0.1$, i.e., based on the difference between the potentials of the oxidation and the first and second reductions in the CV with an estimated entropy effect subtracted out (~0.1 eV).

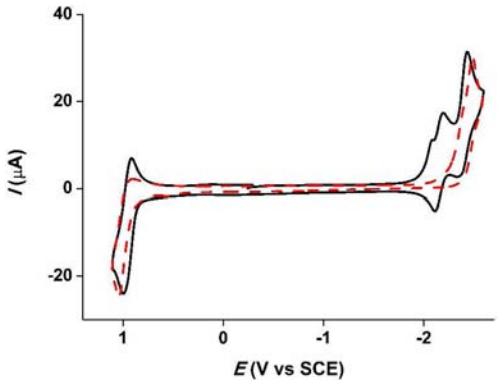

Figure 4. Comparison of CVs of **2** before (solid black line) and after (dashed red line) pulsing the potential for several cycles between the oxidation and the second reduction peaks (+1.1 and −2.65 V vs SCE; DMF/0.1 M TBAH; scan rate, 0.1 V/s).

Upon comparison of the values of E_s and $-\Delta H_{ann}$, as shown in Table 3, we can conclude that for all compounds the annihilation process follows the S-route ($-\Delta H_{ann} > E_s$). The light emission generated by the reaction of radical cations and anions occurs via singlet−singlet annihilation, as the energy difference between the oxidation and the reduction is larger than the energy required to populate the singlet excited state directly.[1−4] The three molecules can be defined as energy-sufficient systems. With a large Stokes shift, a more correct calculation of the energy of the excited singlet state energy can be estimated from the crossing point between the absorption and the emission spectra; in our case, this would yield an excited singlet state energy of 3.02 eV (at 411 nm for **2**), for which our estimated $-\Delta H_{ann}$ = 3.01 eV for oxidation and first reduction would be insufficient to populate it.

Experimentally, we observe that, upon pulsing into the second reduction peak, where $-\Delta H_{ann} \approx 3.29$ eV, the ECL emission profile is maintained (*vide infra* Figure 8b), suggesting that the same excited state is formed and is thus energy-sufficient, even for the oxidation and first reduction case. Given the apparent high ECL efficiency, even with the uncertainties presented in the calculations, we assign it to an energy-sufficient system by considering the maximum of the PL emission, as is usually done for ECL systems.[8,22]

The ECL emission of **1** and **2** superimposed to the corresponding PL is depicted in Figures 5 and 6, respectively. The component of ECL emission at higher energy could be associated with the radiative decay of the singlet excited state. The lower energy band could originate from the formation of side products and excimers or by triplet states.

To rule out possible emission from the triplet states, we performed phosphorescence measurements at 77 K in a methylcyclohexane matrix. Figure 7 depicts the structured

dx.doi.org/10.1021/ja3054018 | J. Am. Chem. Soc. 2012, 134, 15402−15409

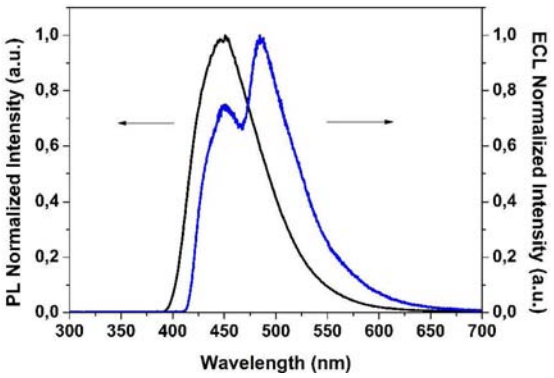

Figure 5. PL (black) and ECL (blue) spectra of **1** in DMF/0.1 M TBAH.

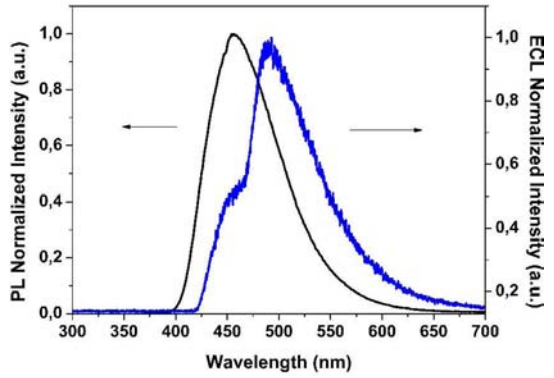

Figure 6. PL (black) and ECL (blue) spectra of **2** in DMF/0.1 M TBAH.

phosphorescence spectra for **1** and **2** and clearly shows that the phosphorescence maxima are at lower energy (λ_{max} = 535 nm) for both compounds than the ECL lowest energy maximum. We can therefore conclude that the low-energy emissions observed in the ECL are not attributed to triplet state deactivations.

To ensure that the feature of the ECL spectrum was not due to excimer formation,[30] BPO was employed as the coreactant, and the potential was scanned only in the negative bias. Unexpectedly, the shape of the emission spectra for all compounds did not show any difference. This is a very surprising result, especially in the case of **1**, because the formation of excimers and their ECL emission was already investigated in many fluorene-based compounds.[31] As reported in the literature,[4] the intensity of ECL emission increases remarkably in the presence of BPO. This behavior is observed for all the three compounds. In particular, ECL of **3** with BPO has been well detected with a shoulder at 465 nm and a maximum at 488 nm (Figure S2, Supporting Information), showing a shape very similar to that of **2**. Although the ECL arising in the presence of the coreactant is not decisive, it strongly suggests that the formation of an excimer is not the reason for the band peaked at about 490 nm in the spectra of all three compounds.[22a] Moreover, the formation of aggregates due to the high concentrations used in the electrochemical experiments is also excluded. In fact, the PL emission profile is maintained in a concentrated solution (10^{-3} M) in the presence of the electrolyte, even when exciting at a longer wavelength (430 nm) where the absorbance is very low (see Figure S3, Supporting Information). Besides, the PL spectra of thin films of **1** and **2** (see Figure S4, Supporting Information) indicate the lack of emission at longer wavelengths also in the solid state. We can then hypothesize that the ECL emission of these compounds arises from the radiative decay of the singlet excited state together with a contribution from a side product formed after pulsing the potential (*vide supra*). However, we cannot exclude a contribution to the ECL emission by the presence of polarons and/or bipolarons and their recombination.[32,33] Further investigations in this direction, which are now beyond the aim of this work, will be taken into consideration for future experiments.

Furthermore, we investigated the effect of the concentration of radical ions in annihilation process. By pulsing selectively between the oxidation peak E_{ox} and $E_{1,red}$ or $E_{2,red}$ potential (+1.2 and −2.3/−2.7 V for **1**, and +1.1 and −2.2/−2.65 V for **2**), an increasing ECL intensity occurred for all the compounds, as shown in Figure 8. This behavior could be explained by taking into account the stoichiometry of radical ions present in solution.[8,22a] In fact, in the positive bias the radical dication is formed, whereas while pulsing in the negative bias, the monoanion or dianion is produced selectively. Pulsing between the oxidation and the first reduction peak results in an excess of radical cation in solution, thus a lower concentration of emitting species. When the spectrum is collected with the second reduction peak, the stoichiometry of radical ions is balanced, and the annihilation reaction of the dication−dianion pair produces a higher intensity ECL emission.

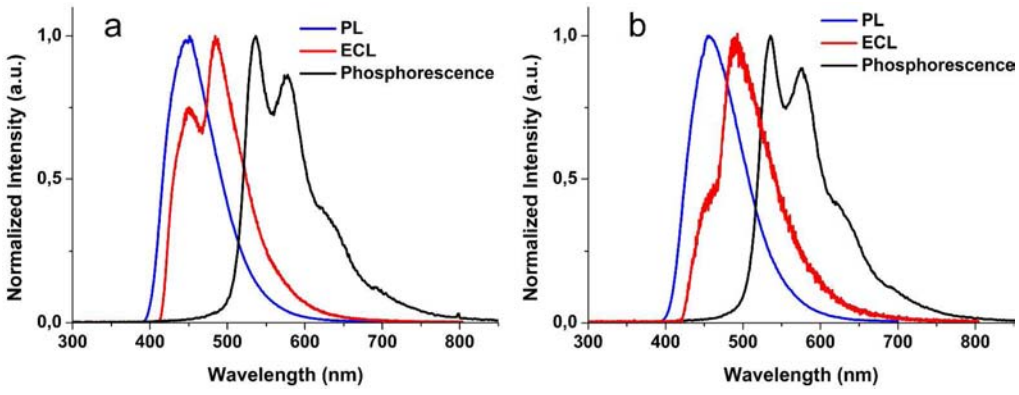

Figure 7. Normalized PL, ECL, and phosphorescence spectra for **1** (a) and **2** (b).

dx.doi.org/10.1021/ja3054018 | J. Am. Chem. Soc. 2012, 134, 15402−15409

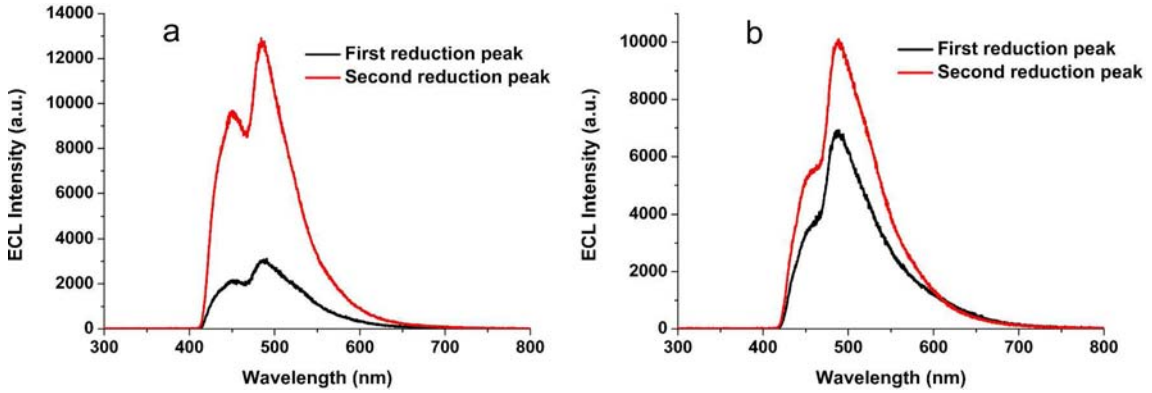

Figure 8. ECL spectra of (a) **1** and (b) **2** collected by pulsing between the oxidation and the first (black) or second (red) reduction peaks.

CONCLUSION

We have reported electrochemical and photophysical behavior of efficient ECL-emitting spirobifluorene- and fluorene-based molecules bearing triphenylamine as substituents. In solution all the compounds showed blue emission with high quantum yields upon photoexcitation and ECL emission in the greenish blue region, resulting in higher efficiency than that of the standard 9,10-diphenylanthracene. The most efficient molecules, i.e., **1** and **2**, have been carefully analyzed from the photophysical and electrochemical points of view in order to understand the origin of the bands that occurred in the ECL spectra. The coreactant approach using BPO generated more intense ECL emission in all molecules (also in **3**) compared to the ion annihilation pathway. However, unlike observations for many other fluorene-based compounds reported in the literature, no change is observed in the shape of ECL spectra produced by reduction in the presence of BPO coreactant. We can suppose that the ECL emission arose from two components, i.e., the singlet excited state obtained by the S-route and a side product formed by scanning potential between anodic and cathodic sweeps. In conclusion, the investigated molecules demonstrate the possibility to design highly blue-emitting systems for ECL applications.

ASSOCIATED CONTENT

Supporting Information

Detailed synthetic procedure for all compounds; ECL photocurrent of **2**; coreactant ECL emission of **3**; and PL spectra of **2** in highly concentrated solution excited at different wavelengths. This material is available free of charge via the Internet at http://pubs.acs.org.

AUTHOR INFORMATION

Corresponding Author

federico.polo@unipd.it; fabio.rizzo@istm.cnr.it

Present Address

[‖]Dipartimento di Scienze Chimiche, Università degli Studi di Padova, Via Marzolo 1, I-35131 Padova, Italy

Notes

The authors declare no competing financial interest.

ACKNOWLEDGMENTS

The authors thank Dr. Gregorio Bottaro of ISTM−CNR of Padova for the PL measurements of concentrated solutions. Financial support by FIRB project RBAP114AMK "Integrated network for nanomedicine−RINAME" of MIUR is also acknowledged.

REFERENCES

(1) *Electrogenerated Chemiluminescence*; Bard, A. J., Ed.; Marcel Dekker: New York, 2004.

(2) Richter, M. M. *Chem. Rev.* **2004**, *104*, 3003−3036 and references therein.

(3) Hu, L.; Xu, G. *Chem. Soc. Rev.* **2010**, *39*, 3275−3304 and references therein. Guo, Z.; Hao, T.; Shi, L.; Gai, P.; Duan, J.; Wang, S.; Gan, N. *Food Chem.* **2012**, *132*, 1092−1097. Joshi, T.; Barbante, G. J.; Francis, P. S.; Hogan, C. F.; Bond, A. M.; Spiccia, L. *Inorg. Chem.* **2011**, *50*, 12172−12183. Ge, L.; Yan, J.; Song, X.; Yan, M.; Ge, S.; Yu, J. *Biomaterials* **2012**, *33*, 1024−1031.

(4) Miao, W. *Chem. Rev.* **2008**, *108*, 2506−2553 and references therein.

(5) Santa Cruz, T. D.; Akins, D. L.; Birke, R. L. *J. Am. Chem. Soc.* **1976**, *98*, 1677−1682.

(6) (a) Bezman, R.; Faulkner, L. R. *J. Am. Chem. Soc.* **1972**, *94*, 6317−6323. (b) Wallace, W. L.; Bard, A. J. *J. Phys. Chem.* **1979**, *83*, 1350−1357.

(7) For example: (a) Omer, K. M.; Ku, S.-Y.; Wong, K.-T.; Bard, A. J. *Angew. Chem., Int. Ed.* **2009**, *48*, 9300−9303. (b) Maness, K. M.; Wightman, R. M. *J. Electroanal. Chem.* **1995**, *396*, 85−95. (c) Booker, C.; Wang, X.; Haroun, S.; Zhou, J.; Jennings, M.; Pagenkopf, B. L.; Ding, Z. *Angew. Chem., Int. Ed.* **2008**, *47*, 7731−7735.

(8) Shen, M.; Rodríguez-López, J.; Huang, J.; Liu, Q.; Zhu, X.-H.; Bard, A. J. *J. Am. Chem. Soc.* **2010**, *132*, 13453−13461.

(9) Zanarini, S.; Felici, M.; Valenti, G.; Marcaccio, M.; Prodi, L.; Bonacchi, S.; Contreras-Carballada, P.; Williams, R. M.; Feiters, M. C.; Nolte, R. J. M.; De Cola, L.; Paolucci, F. *Chem.—Eur. J.* **2011**, *17*, 4640−4647.

(10) For example: (a) Suk, J.; Cheng, J.-Z.; Wong, K.-T.; Bard, A. J. *J. Phys. Chem. C* **2011**, *115*, 14960−14968. (b) Omer, K. M.; Ku, S.-Y.; Cheng, J.-Z.; Chou, S.-H.; Wong, K.-T.; Bard, A. J. *J. Am. Chem. Soc.* **2011**, *133*, 5492−5499. (c) Omer, K. M.; Ku, S.-Y.; Wong, K.-T.; Bard, A. J. *J. Am. Chem. Soc.* **2009**, *131*, 10733−10741.

(11) Rizzo, F.; Cavazzini, M.; Righetto, S.; De Angelis, F.; Fantacci, S.; Quici, S. *Eur. J. Org. Chem.* **2010**, 4004−4016.

(12) (a) Saragi, T. P. I.; Spehr, T.; Siebert, A.; Fuhrmann-Lieker, T.; Salbeck, J. *Chem. Rev.* **2007**, *107*, 1011−1065 and references therein. (b) Liao, Y.-L.; Lin, C.-Y.; Wong, K.-T.; Hou, T.-H.; Hung, W.-Y. *Org. Lett.* **2007**, *9*, 4511−4514. (c) Choi, I. W., ; Kim, C. S.; Kwon, H.-J.; Cho, Y.-J.; Kim, B.-O.; Kim, S.-M.; Yoon, S. S., Gracel Display Inc. Luminescent Compounds and Electroluminescent Device Using the Same. WIPO Patent 2009066815, May 28, 2009. (d) Poriel, C.; Rault-Berthelot, J.; Thirion, D.; Barrière, F.; Vignau, L. *Chem.—Eur. J.* **2011**, *17*, 14031−14046.

(13) (a) Heredia, D.; Natera, J.; Gervaldo, M.; Otero, L.; Fungo, F.; Lin, C.-Y.; Wong, K. T. *Org. Lett.* **2010**, *12*, 12−15. (b) Cho, N.; Choi,

H.; Kim, D.; Song, K.; Kang, M.-S.; Kang, S. O.; Ko, J. *Tetrahedron* **2009**, *65*, 6236−6243.
(14) (a) Wu, C. C.; Lin, Y. T.; Chiang, H. H.; Cho, T. Y.; Chen, C. W.; Wong, K. T.; Liao, Y. L.; Lee, G. H.; Peng, S. M. *Appl. Phys. Lett.* **2002**, *81*, 577−579. (b) Schwartz, G.; Fehse, K.; Pfeiffer, M.; Walzer, K.; Leo, K. *Appl. Phys. Lett.* **2006**, *89*, 083509−511. (c) Chiang, C.-L.; Wu, M.-F.; Dai, D.-C.; Wen, Y.-S.; Wang, J.-K.; Chen, C.-T. *Adv. Funct. Mater.* **2005**, *15*, 231−238.
(15) (a) Sartin, M. M.; Shu, C.; Bard, A. J. *J. Am. Chem. Soc.* **2008**, *130*, 5354−5360. (b) Rashidnadimi, S.; Hung, T. H.; Wong, K.-T.; Bard, A. J. *J. Am. Chem. Soc.* **2008**, *130*, 634−639.
(16) Hosokawa, C.; Funehashi, M.; Kawamura, H.; Arai, H.; Koga, H.; Ikeda, H., Idemitsu Kosan Company Ltd. Organic Electroluminescent Element. Eur. Pat. Appl. 1061112, 2000.
(17) (a) So, H.; Watanabe, H.; Yahiro, M.; Yang, Y.; Oki, Y.; Adachi, C. *Opt. Mater.* **2011**, *33*, 755−758. (b) Komino, T.; Nomura, H.; Yahiro, M.; Endo, K.; Adachi, C. *J. Phys. Chem. C* **2011**, *115*, 19890−19896.
(18) Togushi, S.; Oda, A.; Ishikawa, H., NEC Corp. Organic Thin Film Transistor. U.S. Patent 2003111692, June 19, 2003.
(19) Saroja, G.; Pingzhu, Z.; Ernsting, N. P.; Liebscher, J. *J. Org. Chem.* **2004**, *69*, 987−990.
(20) Yu, W.-L.; Pei, J.; Huang, W.; Heeger, A. J. *Adv. Mater.* **2000**, *12*, 828−831.
(21) Pei, J.; Ni, J.; Zhou, X.-H.; Cao, X.-Y.; Lai, Y.-H. *J. Org. Chem.* **2002**, *67*, 4924−4938.
(22) (a) Shen, M.; Rodríguez-López, J.; Lee, Y.-T.; Chen, C.-T.; Fan, F.-R. F.; Bard, A. J. *J. Phys. Chem. C* **2010**, *114*, 9772−9780. (b) Omer, K. M.; Ku, S.-Y.; Chen, Y.-C.; Wong, K.-T.; Bard, A. J. *J. Am. Chem. Soc.* **2010**, *132*, 10944−10952.
(23) Vonlanthen, D.; Rudnev, A.; Mishchenko, A.; Käslin, A.; Rotzler, J.; Neuburger, M.; Wandlowski, T.; Mayor, M. *Chem.—Eur. J.* **2011**, *17*, 7236−7250.
(24) Bard, A. J.; Faulkner, L. R. *Electrochemical Methods, Fundamentals and Applications*, 2nd ed.; John Wiley & Sons: New York, 2001.
(25) Valeur, B. *Molecular Fluorescence: Principles and Applications*; Wiley-VHC: Weinheim, Germany, 2001.
(26) Promarak, V.; Ichikawa, M.; Sudyoadsuk, T.; Saengsuwan, S.; Keawin, T. *Opt. Mater.* **2007**, *30*, 364−369.
(27) Fungo, F.; Wong, K.-T.; Ku, S.-Y.; Hung, Y.-Y.; Bard, A. J. *J. Phys. Chem. B* **2005**, *109*, 3984−3989.
(28) Maness, K. M.; Bartelt, J. E.; Wightman, R. M. *J. Phys. Chem.* **1994**, *98*, 3993−3998.
(29) (a) Seo, E. T.; Nelson, R. F.; Fritsch, J. M.; Marcoux, L. S.; Leedy, D. W.; Adams, R. N. *J. Am. Chem. Soc.* **1968**, *90*, 3498−3503. (b) Nelson, R. F.; Adams, R. N. *J. Am. Chem. Soc.* **1968**, *90*, 3925−3930. (c) Otero, L.; Sereno, L.; Fungo, F.; Liao, Y.-L.; Lin, C.-Y.; Wong, K.-T. *Chem. Mater.* **2006**, *18*, 3495−3502.
(30) Choi, J.-P.; Wong, K.-T.; Chen, Y.-M.; Yu, J.-K.; Chou, P.-T.; Bard, A. J. *J. Phys. Chem. B* **2003**, *107*, 14407−14413.
(31) Prieto, I.; Teetsov, J.; Fox, M. A.; Vanden Bout, D. A.; Bard, A. J. *J. Phys. Chem. A* **2001**, *105*, 520−523.
(32) Burrows, H. D.; Seixas de Melo, J.; Forster, M.; Güntner, R.; Scherf, U.; Monkman, A. P.; Navaratnam, S. *Chem. Phys. Lett.* **2004**, *385*, 105−110.
(33) Zaikowski, L.; Kaur, P.; Gelfond, C.; Selvaggio, E.; Asaoka, S.; Wu, Q.; Chen, H.-C.; Takeda, N.; Cook, A. R.; Yang, A.; Rosanelli, J.; Miller, J. R. *J. Am. Chem. Soc.* **2012**, *134*, 10852−10863.